THE JOURNAL OF BIOLOGICAL CHEMISTRY VOL. 284, NO. 40, pp. 27596–27608, October 2, 2009

NEMO-binding Domains of Both IKKα and IKKβ Regulate IκB Kinase Complex Assembly and Classical NF-κB Activation*

Received for publication, July 21, 2009 Published, JBC Papers in Press, August 7, 2009, DOI 10.1074/jbc.M109.047563

Laura A. Solt[‡], **Lisa A. Madge**[‡], **and Michael J. May**[‡§1]

From the [‡]*Department of Animal Biology and the* [§]*Mari Lowe Center for Comparative Oncology, University of Pennsylvania School of Veterinary Medicine, Philadelphia, Pennsylvania 19104*

Proinflammatory NF-κB activation requires the IκB (inhibitor of NF-κB) kinase (IKK) complex that contains two catalytic subunits named IKKα and IKKβ and a regulatory subunit named NF-κB essential modulator (NEMO). NEMO and IKKβ are essential for tumor necrosis factor (TNF)-induced NF-κB activation, and we recently demonstrated that NEMO and IKKα are sufficient for interleukin (IL)-1-induced signaling. IKKα and IKKβ both contain a functional NEMO-binding domain (NBD); however, the role of NEMO association with each kinase in NF-κB signaling and IKK complex formation remains unclear. To address this question, we stably reconstituted IKK$\alpha^{-/-}$ and IKK$\beta^{-/-}$ murine embryonic fibroblasts (MEFs) with wild-type (WT) or NBD-deficient (ΔNBD) versions of IKKα and IKKβ, respectively. TNF-induced classical NF-κB activation in IKK$\beta^{-/-}$ MEFs was rescued by IKKβ^{WT} but not IKK$\beta^{\Delta NBD}$, whereas neither IKKβ^{WT} nor IKK$\beta^{\Delta NBD}$ affected IL-1-induced NF-κB signaling. As previously described, classical NF-κB transcriptional activity was absent in IKK$\alpha^{-/-}$ cells. Reconstitution with either IKKα^{WT} or IKK$\alpha^{\Delta NBD}$ rescued both IL-1 and TNF-induced transcription, demonstrating that NEMO association is not required for IKKα-dependent regulation of NF-κB-dependent transcription. Stably expressed IKKα^{WT} or IKKβ^{WT} associated with endogenous IKKs and NEMO in IKK$\alpha^{-/-}$ or IKK$\beta^{-/-}$ MEFs, respectively, resulting in formation of the heterotrimeric IKKα-IKKβ-NEMO complex. In contrast, although the IKK$\alpha^{\Delta NBD}$ and IKK$\beta^{\Delta NBD}$ mutants associated with endogenous IKKs containing an NBD, these dimeric endogenous IKK-IKK$^{\Delta NBD}$ complexes did not associate with NEMO. These findings therefore demonstrate that formation of the heterotrimeric IKKα-IKKβ-NEMO holocomplex absolutely requires two intact NEMO-binding domains.

NF-κB[2] describes a family of transcription factors that regulate the inducible expression of many genes essential for innate and adaptive immunity, inflammation, and cell survival. A wide range of stimuli activates NF-κB, including ligation of innate immune receptors (*e.g.* TLRs), antigen receptor engagement (B cell receptor and T cell receptor), and proinflammatory cytokines (*e.g.* IL-1 and TNF) (1). NF-κB activation by these stimuli is normally rapid and transient; however, constitutive NF-κB activity occurs in some chronic inflammatory diseases, solid tumors, leukemias, and lymphomas (1, 2). Understanding the molecular mechanisms that regulate NF-κB activity will therefore reveal novel targets for blocking pathophysiological NF-κB signaling (3–5).

The five NF-κB family members are NF-κB1/p105 and NF-κB2/p100 that are processed to generate p50 and p52, respectively, p65 (RelA), c-Rel, and RelB (1). These proteins homo- or heterodimerize to form transcriptionally active (*e.g.* p50-p65) or repressive (*e.g.* p50-p50) dimers that are retained in the cytosol of resting cells by members of the inhibitory family of IκB proteins. The IκBs include IκBα, IκBβ, IκBϵ, and the C termini of p105 and p100. The prototypic NF-κB-IκB complex expressed in most cell types is a heterodimer of p50 and p65 associated with IκBα (1). Following cell stimulation, the IκBs are rapidly phosphorylated, ubiquitinated, and then degraded by the 26 S proteasome. Free NF-κB dimers then migrate to the nucleus, where they bind target gene promoters and regulate transcription (1).

The IκB proteins are phosphorylated by the high molecular weight heterotrimeric IκB (inhibitor of NF-κB) kinase (IKK) complex (1, 6, 7). The IKK complex contains two kinases named IKKα (IKK1) and IKKβ (IKK2) and a noncatalytic subunit named NEMO (NF-κB essential modulator) or IKKγ (1, 6, 7). NEMO is critical for proinflammatory IKK activation (8–12), and we previously identified a domain within the C termini of both IKKα and IKKβ that facilitates their association with NEMO (13, 14). A cell-permeable peptide spanning this NEMO-binding domain (NBD) disrupts the IKK complex and blocks proinflammatory NF-κB activation, confirming the crucial role of NEMO association for IKK complex activation (13).

Despite their significant structural similarities, genetic analyses of IKKα and IKKβ revealed distinct roles for the kinases during NF-κB activation (1, 6, 7, 15). In this regard, TNF-induced IκBα degradation is dependent upon IKKβ and also requires NEMO (8, 16, 17). This mechanism is termed the classical NF-κB pathway and is defined as NEMO- and IKKβ-dependent IκB phosphorylation and degradation releasing canonical NF-κB complexes typified by the ubiquitous p50-p65 heterodimer. IKKα plays a separate role in mediating NIK (NF-κB-inducing kinase)-dependent processing of NF-κB2/p100 to generate p52 (18–22). This mechanism is activated in the absence of both IKKβ and NEMO and is named the noncanoni-

* This work was supported, in whole or in part, by National Institutes of Health Grants 1RO1-HL-080612 and T32-AI-055428-06. This work was also supported by W. W. Smith Charitable Trust Grant H0703.

[1] To whom correspondence should be addressed: Dept. of Animal Biology, University of Pennsylvania School of Veterinary Medicine, 3800 Spruce St. (OVH 200E), Philadelphia, PA 19104. Tel.: 215-573-0940; Fax: 215-573-5186; E-mail: maym@vet.upenn.edu.

[2] The abbreviations used are: NF-κB, nuclear factor-κB; IKK, IκB kinase; MEF, murine embryonic fibroblast; NBD, NEMO-binding domain; IL, interleukin; TNF, tumor necrosis factor; WT, wild type; FACS, fluorescence-activated cell sorting; EMSA, electrophoretic mobility shift assay.

cal NF-κB pathway (15). Ligation of only a subset of receptors, including the lymphotoxin-β receptor, CD40, and BAFF-R, activates the IKKα-dependent noncanonical pathway, and the resulting p52, together with RelB, regulates a panel of chemokine and cytokine genes required for lymphoid organogenesis and B-cell maturation (18–23). IKKα has also been shown to play several roles in regulating the transcriptional activity of classical NF-κB that are separate from its upstream signaling function as an IκB kinase (24–29).

Since TNF-induced IκBα degradation and classical NF-κB nuclear translocation occurs in the absence of IKKα, a model of classical pathway activation has emerged in which IKKα is redundant (15). It remains, however, that IKKα associates via its NBD with NEMO (14), and we previously questioned whether this association plays a functional role in classical NF-κB signaling (30). Surprisingly, we found that although TNF-induced IκBα degradation requires NEMO and IKKβ, IL-1-induced classical pathway activation is intact in cells lacking IKKβ. Furthermore, IL-1-induced NF-κB activation in IKKβ-deficient cells was blocked by the NBD peptide, demonstrating that a complex of only IKKα and NEMO is sufficient for IL-1- but not TNF-induced classical NF-κB activation (30). Intriguingly, Lam *et al.* (31) recently demonstrated that IKKα plays a crucial compensatory role in regulating constitutive classical NF-κB pathway activation in a subset of diffuse large B-cell lymphoma cells in which IKKβ has been pharmacologically inhibited. These findings therefore identify differences in the absolute requirements for the separate IKK subunits activated in a NEMO-dependent manner by distinct stimuli and suggest that targeting only IKKβ may not effectively block dysregulated classical NF-κB activation. Consequently, determining the role of the interaction of each IKK subunit with NEMO will provide novel insight into the mechanisms that regulate NEMO-dependent classical NF-κB activation.

To address this question, we determined the effects of individually deleting the NBD in IKKα and IKKβ on classical NF-κB signaling and IKK complex formation. We stably reconstituted IKK$\alpha^{-/-}$ and IKK$\beta^{-/-}$ murine embryonic fibroblasts (MEFs) with wild-type (WT) or NBD-deficient (ΔNBD) versions of IKKα and IKKβ, respectively. Reconstitution of IKK$\beta^{-/-}$ MEFs with IKKβ^{WT} but not IKK$\beta^{\Delta NBD}$ rescued TNF-induced classical NF-κB activation, confirming the requirement for the NEMO-IKKβ association for TNF signaling. IL-1 signaling was intact in IKK$\beta^{-/-}$ cells, and this was not affected by expression of either IKKβ^{WT} or IKK$\beta^{\Delta NBD}$. Classical NF-κB transcriptional activity was absent in IKK$\alpha^{-/-}$ cells, and reconstitution with either IKKα^{WT} or IKK$\alpha^{\Delta NBD}$ rescued both IL-1- and TNF-induced transcription. This therefore demonstrates that association with NEMO is not necessary for IKKα-dependent regulation of NF-κB-dependent transcriptional activity. Immunoprecipitation analysis and size exclusion chromatography revealed that stably expressed IKKα^{WT} or IKKβ^{WT} associated with endogenous IKKs and NEMO in IKK$\alpha^{-/-}$ or IKK$\beta^{-/-}$ MEFs, respectively. This association resulted in the formation of the heterotrimeric IKKα-IKKβ-NEMO complex. In contrast, despite the ability of the IKK$\alpha^{\Delta NBD}$ and IKK$\beta^{\Delta NBD}$ mutants to associate with endogenous IKKs containing an NBD, these mutants formed dimeric endogenous IKK-IKK$^{\Delta NBD}$ complexes that did not associate with NEMO. These findings therefore demonstrate that formation of the heterotrimeric IKKα-IKKβ-NEMO holocomplex absolutely requires the presence of two intact NEMO-binding domains.

EXPERIMENTAL PROCEDURES

Reagents and Cell Culture—Recombinant human IL-1α was obtained from Peprotech (Rocky Hill, NJ). Recombinant human TNF and recombinant mouse LTα1β2 were from R&D Systems (Minneapolis, MN). Polyclonal rabbit anti-IKKα (sc-7218), rabbit anti-NEMO (sc-8330), goat anti-NEMO (sc-8256), rabbit anti-p100/p52 (sc-298), and rabbit anti-IKKβ (sc-8014) antisera were from Santa Cruz Biotechnology, Inc. (Santa Cruz, CA). Monoclonal anti-α-tubulin (T5168) was from Sigma. Anti-phospho-p65 (Ser^{536}) (catalog number 3033), anti-phospho-IKKα/β (Ser$^{176/180}$) (catalog number 2694), and anti-histone 3 (catalog number 9715) were from Cell Signaling Technologies (Beverly, MA). Normal rabbit IgG (sc-2027), normal goat IgG (sc-2028), and donkey anti-mouse IgG (sc-2518), used as nonspecific antibodies in immunoprecipitations, were from Santa Cruz Biotechnology. Immobilized Protein A/G beads were from Pierce, and Protein G-Sepharose beads were from Amersham Biosciences. Horseradish peroxidase-conjugated secondary antibodies against either rabbit or mouse IgG, AffiniPure goat anti-mouse IgG light chain-specific, and IgG fraction monoclonal mouse anti-rabbit IgG light chain-specific secondary antibodies were from Jackson ImmunoResearch Laboratories (West Grove, PA).

WT, IKK$\alpha^{-/-}$, and IKK$\beta^{-/-}$ MEFs were generously provided by Dr. Inder Verma (Salk Institute for Biological Studies, La Jolla, CA). Plat-E cells were kindly provided by Dr. Tadaichi Kitamura (Institute of Medical Science, University of Tokyo, Japan), and Phoenix cells were provided by Dr. Garry Nolan (Stanford University, Stanford, CA). All cells were maintained in Dulbecco's modified Eagle's medium (Invitrogen) supplemented with 10% fetal calf serum, 2 mM L-glutamine, penicillin (50 units/ml), and streptomycin (50 μg/ml). For all experiments, unless otherwise indicated, cells were cultured in either 6-well tissue culture trays or 100-mm dishes and were stimulated with IL-1α (10 ng/ml) or TNF (10 ng/ml) when they reached 80% confluence.

Generation of Stable Cell Lines—All cloning procedures were performed by PCR using cloned *Pfu* DNA polymerase (Stratagene, La Jolla, CA). Complementary DNA encoding full-length IKKβ or IKKβ 1–733 (IKK$\beta^{\Delta NBD}$) were subcloned into the HindIII and NotI sites of the LZRS-pBMN-lacZ retroviral vector (kindly provided by Dr. Garry Nolan). Resulting LZRS-IKKβ^{WT} and LZRS-IKK$\beta^{\Delta NBD}$ were transiently transfected using Fugene6 into Phoenix cells and selected for gene expression 24 h after transfection using puromycin (1 μg/ml). Puromycin-resistant cells were used to derive conditioned medium to provide a retroviral stock for MEF transduction. For cell transduction, IKK$\beta^{-/-}$ MEFs were washed and incubated for 8 h with retrovirus-conditioned medium containing Polybrene (8 μg/ml; Sigma). After incubation, retrovirus was removed and replaced with normal growth medium. The transduction process was repeated a further three times until cells became positive for IKKβ when visualized by immunoblotting.

To generate stably transduced IKKα^{WT} and IKKα$^{\Delta NBD}$ MEFs, full-length IKKα or IKKα$^{\Delta NBD}$ cDNA was cloned into the EcoRI and XhoI restriction sites of retroviral GFP-MIGR1 vector (kindly provided by Dr. Warren Pear, University of Pennsylvania, Philadelphia, PA). The resulting MIG-IKKα^{WT} and MIG-IKKα$^{\Delta NBD}$ were transiently transfected using Fugene6 into Plat-E cells to produce ecotropic virus that was derived from conditioned medium containing Polybrene (8 μg/ml). For cell transduction, IKKα$^{-/-}$ MEFs were washed and incubated for 8 h with retrovirus-conditioned medium. After incubation, retrovirus was removed and replaced with normal growth medium. The transduction process was repeated a further three times until cells became positive for IKKα, as assessed by FACS analysis using Cell Quest software (FACSort; BD Biosciences).

For cell sorting, transduced cells were trypsinized and washed in FACS buffer (sterile phosphate-buffered saline, 0.5 M EDTA, and 0.5% bovine serum albumin). Evaluation of green fluorescent protein was performed on a three-laser (argon (488 nm), krypton (407 nm), and dye laser (tuned to 600 nm)), 10-parameter FACSVantage^{TM} obtained from BD Biosciences. Compensation and data analyses were performed using FlowJo software (Tree Star, Ashland, OR).

Immunoblotting and Immunoprecipitation—Cells were washed once with phosphate-buffered saline and then incubated for 10 min at 4 °C in 100 μl of TNT lysis buffer (50 mM Tris-Cl, pH 7.5, 150 mM NaCl, and 1% Triton X-100) and a complete miniprotease inhibitor mixture (Roche Applied Science). Samples were then scraped and harvested into 1.5-ml microcentrifuge tubes, vortexed for 30 s, and then centrifuged (425 × *g* for 10 min). Protein levels in supernatants were determined using a Coomassie protein assay kit (Bio-Rad), and 20 μg of protein from each sample was separated by SDS-PAGE (10%) then transferred to a polyvinylidene difluoride membrane (Millipore, Milford, MA) and immunoblotted with primary and horseradish peroxidase-conjugated secondary antibodies. Detection of the bound antibody by enhanced chemiluminescence was performed according to the manufacturer's instructions (Pierce). For immunoprecipitations, cell extracts were incubated with 2 μg of primary antibody for 1 h at 4 °C, followed by incubation (1 h/4 °C) with 50 μl of Protein G-Sepharose beads (50% slurry) or 50 μl Protein A/G beads (50% slurry). A portion of each sample preimmunoprecipitation (5%) was retained for analysis. The beads were washed three times with lysis buffer, and then samples were analyzed by SDS-PAGE (10%) followed by immunoblotting, as described above.

Immune Complex Kinase Assay—For immune complex kinase assays, MEF lysates were prepared, and immunoprecipitations were performed as described above. The resulting immunoprecipitates were washed extensively in TNT and then kinase buffer (20 mM HEPES, pH 7.5, 20 mM $MgCl_2$, 1 mM EDTA, 2 mM NaF, 2 mM β-glycerophosphate, 1 mM dithiothreitol, 10 mM ATP). Precipitates were then incubated for 15 min at 30 °C in 20 μl of kinase buffer containing glutathione *S*-transferase-IκBα (amino acids 1–54; a generous gift from Dr. Serge Fuchs, University of Pennsylvania) and 10 μCi of [γ-^{32}P]ATP (Amersham Biosciences). The substrate was then precipitated using glutathione-agarose (Amersham Biosciences) and washed extensively with TNT. Beads were then suspended in 20 μl of sample buffer, and samples were separated by SDS-PAGE (10%). The resulting gel was stained with Coomassie Blue solution (0.05% Brilliant Blue G250, 40% methanol, 10% acetic acid) and then destained (40% methanol, 10% acetic acid) and dried. Kinase activity was determined by autoradiography.

Generation of Nuclear Lysates for Immunoblotting—MEFs were stimulated with TNFα (10 ng/ml) for the indicated times and then scraped into phosphate-buffered saline at 4 °C and pelleted (425 × *g*, 10 min). Pellets were resuspended and swollen for 10 min on ice in 100 μl of Buffer A (10 mM HEPES, pH 7.9, 10 mM KCl, 0.1 mM EDTA, 2 mM NaF, 2 mM β-glycerol phosphate, and complete miniprotease inhibitors) plus 0.1% Nonidet P-40 and centrifuged (3800 × *g*) for 1 min. Supernatants (cytoplasmic fraction) were centrifuged at 20,000 × *g* for 1 h at 4 °C, and the resulting supernatants were snap frozen and retained for analysis. Pelleted nuclei were washed four times with 100 μl of Buffer A plus 0.1% Nonidet P-40 buffer before being lysed in 30 μl of 1% TNT, 1% SDS buffer plus complete mini protease inhibitors with a 26-gauge (half-inch) needle. Nuclear lysates were then centrifuged for 20 min (20,000 × *g*) at room temperature and then either used immediately or snap frozen and stored at −80 °C. Lysates were immunoblotted as described above.

Transfections and Luciferase Reporter Assays—WT MEFs and stable cell lines grown in 12-well plates (2.5 × 10^5/well) were transiently transfected using Fugene6 (Roche Applied Science) following the manufacturer's protocol. Cells were transfected with a total of 0.11 μg of DNA/well, consisting of the NF-κB-dependent firefly reporter construct pBIIx-luciferase (0.2 μg/well) and a *Renilla* luciferase reporter (0.02 μg/ml). Cells were stimulated with TNFα or IL-1α for 5 h and then lysed in passive lysis buffer (Promega, San Luis Obispo, CA) 24–36 h after transfection. Samples were assayed using a Luminoscan 96-well automated luminometer (Thermo Labsystems, Franklin, MA), and firefly/Renilla luciferase ratios were calculated using Ascent software (Thermo LabSystems).

Electrophoretic Mobility Shift Assays (EMSAs)—MEFs were stimulated with TNFα (10 ng/ml) or IL-1α (10 ng/ml) for the indicated times and then scraped into phosphate-buffered saline at 4 °C and pelleted (425 × *g*, 10 min). Pellets were resuspended and swollen for 30 min on ice in 100 μl of Buffer A (10 mM HEPES, pH 7.9, 10 mM KCl, 0.1 mM EDTA, 2 mM NaF, 2 mM β-glycerol phosphate, and complete mini protease inhibitors), incubated a further 5 min on ice in 0.1% Nonidet P-40, and then vortexed and centrifuged (3800 × *g*) for 1 min. Supernatants (cytoplasmic fraction) were centrifuged at 20,000 × *g* for 1 h at 4 °C, and the resulting supernatants were snap-frozen and retained for analysis. Pelleted nuclei were washed once with 100 μl of Buffer A buffer before being vortexed in 30 μl of NarC buffer (20 mM HEPES, pH 7.9, 0.4 M NaCl, pH 8, 1 mM EDTA, pH 8, 2 mM NaF, 2 mM β-glycerol phosphate, and complete mini protease inhibitors) for 1 h at 4 °C. Nuclear lysates were then centrifuged for 20 min (20,000 × *g*) at room temperature and then either used immediately or snap-frozen and stored at −80 °C.

Single-stranded complementary oligonucleotides encompassing a consensus NF-κB site (upper strand, 5′-AGTT-

GAGGGGACTTTCCCAGGC-3′) or the Oct-1 probe (Santa Cruz Biotechnology) were annealed and then labeled with [γ-^{32}P]ATP using T4 PNK (New England Biolabs, Beverly, MA). Labeled probe was purified using mini-Quick Spin columns (Roche Applied Science) according to the manufacturer's instructions. For EMSA, 2–5 μg of nuclear extracts supplemented with 1 μg of poly(dI-dC) (Roche Applied Science) was incubated with an equal volume of 2× binding buffer (40 mM Tris·Cl, pH 7.9, 100 mM NaCl, 10 mM $MgCl_2$, 2 mM EDTA, 20% glycerol, 0.2% Nonidet P-40, 2 mM dithiothreitol, 100 μg/ml bovine serum albumin) on ice for 10 min. After incubation, 1 μl of labeled probe was added, and then samples were incubated at room temperature for 20 min. Resulting DNA-NF-κB complexes were separated on 5% polyacrylamide nondenaturing gels by electrophoresis, and then gels were dried and visualized by autoradiography.

NBD Peptides—NBD peptides were obtained from the Howard Hughes Medical Institute Biopolymer-Keck Foundation Biotechnology Resource Laboratory at Yale University (New Haven, CT). Immediately prior to use, the peptides were dissolved in dimethyl sulfoxide to a stock of 50 mM. The sequences of the wild-type (NBD^{WT}) and mutant (NBD^{MUT}) peptides have been described previously (13, 14). The NBD^{WT} peptide contains the region of IKK-β from Thr^{735} to Glu^{745} synthesized in tandem with a membrane permeabilization sequence from the *Drosophila* antennapedia homeodomain protein. The NBD^{MUT} peptide is identical, except that Trp^{739} and Trp^{741} are replaced by alanines to render it biologically inactive (13, 14).

Fast Protein Liquid Chromatography—Confluent monolayers of MEFs were trypsinized and pelleted after one wash with ice-cold phosphate-buffered saline. To make S100 lysates, cell pellets were swollen on ice for 30 min in 500 μl of lysis buffer (10 mM HEPES, pH 7.9, 10 mM KCl, 0.1 mM EDTA). After 30 min, a final volume 0.1% Nonidet P-40 was added to the swollen pellet, and cells were lysed with 15 strikes of a 2-ml Dounce homogenizer on ice. Finally, one-fourth volume of 5× gel filtration buffer (100 mM Tris, pH 7.5, 50% glycerol, 2.5 mM EDTA, 750 mM NaCl) was added to the lysate before being centrifuged for 10 min at 425 × *g*. The remaining supernatant was then ultracentrifuged 1 h at 100,000 × *g*.

For all size exclusion chromatography procedures, up to 200 μl of S100 lysates was injected onto a Superdex 200 HR 10/30 gel filtration column (Amersham Biosciences). Samples were fractionated with a flow rate of 0.25 ml/min, and 0.5-ml fractions were collected. The gel filtration buffer contained 20 mM Tris (pH 7.5), 10% glycerol, 150 mM NaCl, 0.5 mM EDTA, 20 mM NaF, 20 mM β-glycerophosphate, 1 mM dithiothreitol, 1 mM aprotinin, 1 μM pepstatin, and 10 μM leupeptin. The column was precalibrated using the following standards (Amersham Biosciences): blue dextran (2000 kDa), thyroglobulin (670 kDa), ferritin (440 kDa), catalase (230 kDa), aldolase (158 kDa), and albumin (67 kDa). Fractions 13–31 (containing the IKK complex) were used for immunoblot analysis. In addition, fractions containing the IKK complex were immunoprecipitated using either anti-NEMO or anti-IKKα, and the resulting precipitates were immunoblotted as described above.

RESULTS

The IKKβ NBD Is Required for TNF- but Not IL-1-induced NF-κB Activation—To determine the effects of selectively disrupting the IKKβ-NEMO interaction on classical NF-κB signaling and IKK complex formation, we generated retroviral constructs encoding both WT IKKβ and a truncation mutant (residues 1–733) lacking the NBD (IKKβ$^{\Delta NBD}$) (Fig. 1*A*). We stably transduced IKKβ-deficient MEFs with these constructs and confirmed by immunoblotting that the cells were reconstituted with IKKβ^{WT} and IKKβ$^{\Delta NBD}$ (Fig. 1*B*). FACS analysis verified that over 95% of the cells were stably transduced with each construct (data not shown). The levels of IKKβ^{WT} in multiple cell lines that we generated were consistently higher than endogenous IKKβ in WT MEFs. However, the levels of reconstituted IKKβ$^{\Delta NBD}$ were comparable with endogenous IKKβ levels in WT cells (Fig. 1*B*, compare *lanes 1* and *4*). To examine the effects of reconstituted IKKβ^{WT} and IKKβ$^{\Delta NBD}$ on classical NF-κB activation, we incubated WT, IKKβ$^{-/-}$, IKKβ^{WT}, and IKKβ$^{\Delta NBD}$ MEFs for a range of times with TNF or IL-1 and then immunoblotted the resulting lysates using anti-IκBα. Following cytokine treatment, IκBα degradation and resynthesis was intact in WT MEFs, and consistent with our earlier findings (30), IL-1 but not TNF induced robust IκBα degradation in IKKβ$^{-/-}$ cells (Fig. 1*C*). As expected, TNF-stimulated IκBα degradation was restored in IKKβ^{WT}-reconstituted MEFs (Fig. 1*C*). In contrast, TNF did not induce IκBα degradation in IKKβ$^{\Delta NBD}$-reconstituted cells (Fig. 1*C*), confirming that the IKKβ NBD is required for TNF-induced classical NF-κB pathway activation.

We previously showed that IKK complexes containing NEMO and either IKKα or IKKβ alone could facilitate IL-1-induced IκBα phosphorylation and classical NF-κB activation (30). Since IKKβ has been shown to be a more potent kinase for IκBα that IKKα (32, 33), we questioned whether reconstituting IKKβ$^{-/-}$ MEFs with IKKβ$^{\Delta NBD}$ inhibited or disrupted NEMO-IKKα-dependent IL-1 signaling. As shown in Fig. 1*C* (*right panels*), IL-1-induced IκBα degradation was intact in IKKβ$^{-/-}$ MEFs reconstituted with either IKKβ^{WT} or IKKβ$^{\Delta NBD}$. Furthermore, EMSA analysis demonstrated that the kinetics of IL-1-induced NF-κB nuclear translocation and DNA binding in IKKβ$^{-/-}$, IKKβ^{WT}, and IKKβ$^{\Delta NBD}$ cells were similar to WT MEFs (Fig. 1*D*). Hence, IKKβ$^{\Delta NBD}$ does not block IL-1-induced classical NF-κB activation.

We next examined basal and IL-1-induced NF-κB transcriptional activity in the panel of MEFs using an NF-κB-specific luciferase reporter assay. Consistent with our previous results (30), IL-1 increased NF-κB activity in IKKβ$^{-/-}$ MEFs to a similar level as that observed in WT cells (Fig. 1*E*). Both basal and IL-1-stimulated levels of NF-κB activity were slightly enhanced in IKKβ^{WT}-reconstituted MEFs, possibly due to the higher levels of IKKβ expression in these cells compared with WT MEFs (Fig. 1*B*). However, basal and IL-1-induced NF-κB-dependent transcriptional activity was enhanced in IKKβ$^{\Delta NBD}$ MEFs (Fig. 1*E*) that contained levels of IKKβ$^{\Delta NBD}$ comparable with WT MEFs (Fig. 1*B*). This finding is consistent with our previous observation of enhanced NF-κB activation in HeLa cells transiently overexpressing NEMO-binding mutants of IKKβ (13,

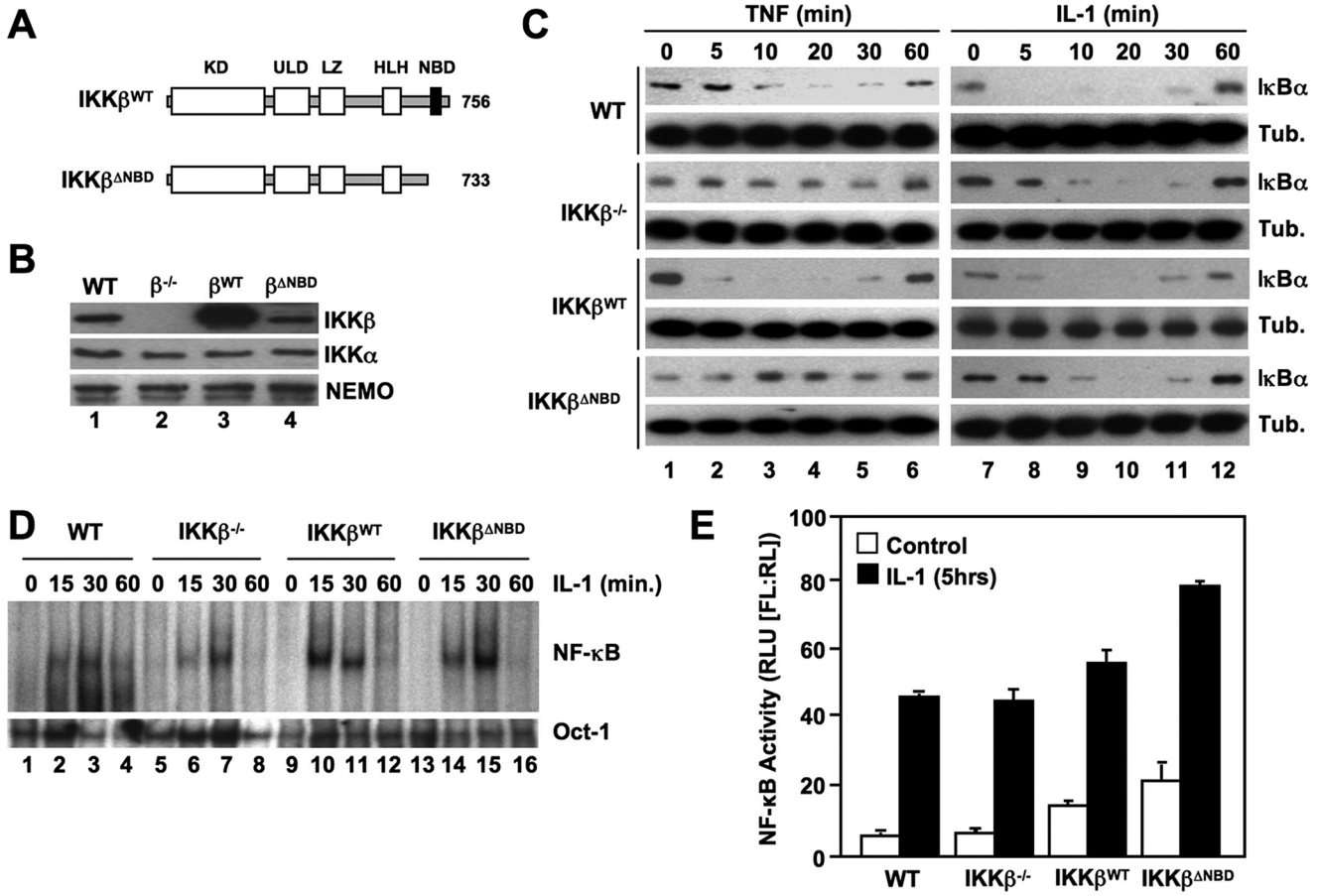

FIGURE 1. **The IKKβ NBD is required for TNF- but not IL-1-induced classical NF-κB activation.** *A*, the structural domains of wild-type IKKβ (IKKβ^{WT}) and IKKβ$^{\Delta NBD}$ are shown. *KD*, kinase domain; *LZ*, leucine zipper; *ULD*, ubiquitin-like domain; *HLH*, helix-loop-helix. IKKβ$^{\Delta NBD}$ is a truncation mutant encompassing residues 1–733 that lacks the C-terminal 23 amino acids containing the NBD (13, 14). *B*, lysates from WT, IKKβ$^{-/-}$ (β$^{-/-}$), IKKβ^{WT} (β^{WT}), and IKKβ$^{\Delta NBD}$ (β$^{\Delta NBD}$) MEFs were immunoblotted using the antibodies indicated (*right*). *C*, WT, IKKβ$^{-/-}$, IKKβ^{WT}, and IKKβ$^{\Delta NBD}$ MEFs were incubated with either TNF (10 ng/ml) (*left*) or IL-1α (10 ng/ml) (*right*) for the times indicated, and then lysates were immunoblotted using anti-IκBα or anti-tubulin (*Tub.*) as a loading control. *D*, the same panel of MEFs was treated with IL-1α for the indicated times, and then nuclear extracts were prepared for EMSA. Assays were performed using either a consensus NF-κB binding site probe (*top*) or an Oct-1 probe as a loading control (*bottom*). *E*, MEFs were transiently transfected with the NF-κB-dependent reporter pBIIx-firefly luciferase together with β-actin *Renilla* luciferase. Twenty-four hours later, cells were either left untreated or treated for a further 5 h with IL-1α, and then NF-κB activity was determined by a dual luciferase assay.

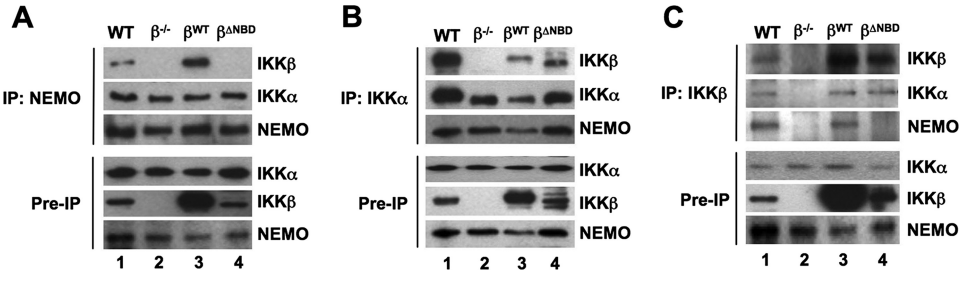

FIGURE 2. **IKKβ$^{\Delta NBD}$ associates with endogenous IKKα but not with endogenous NEMO.** IKK complexes in whole cell lysates of WT, IKKβ$^{-/-}$ (β$^{-/-}$), IKKβ^{WT} (β^{WT}), and IKKβ$^{\Delta NBD}$ (β$^{\Delta NBD}$) MEFs were immunoprecipitated (*IP*) using anti-NEMO (*A*), anti-IKKα (*B*), or anti-IKKβ (*C*). Immunoprecipitated material was immunoblotted using anti-IKKα, anti-IKKβ, and anti-NEMO as indicated (*right*). Samples of lysates saved prior to immunoprecipitation (*Pre-IP*) were immunoblotted using anti-IKKα, anti-IKKβ, and anti-NEMO as shown.

14) and supports our earlier conclusion that the IKKβ NBD plays a role in maintaining the basal activity of the IKK complex.

IKKβ$^{\Delta NBD}$ Is Not Incorporated into the IKK Holocomplex—Within the tripartite IKK holocomplex, IKKα and IKKβ interact via their respective leucine zipper domains (34). Each IKK subunit in turn associates via its C-terminal NBD with NEMO (13, 14, 35). We therefore questioned whether IKKβ$^{\Delta NBD}$ was incorporated into a trimeric IKK complex in IKKβ$^{-/-}$ MEFs via interaction with endogenous IKKα associated with NEMO. To determine the effects of deleting the IKKβ NBD on complex formation, we immunoprecipitated IKK complexes from WT, IKKβ$^{-/-}$, IKKβ^{WT}, and IKKβ$^{\Delta NBD}$ MEFs using anti-NEMO, anti-IKKα, and anti-IKKβ. As shown in Fig. 2*A*, IKKα and IKKβ both co-immunoprecipitated with NEMO from WT and IKKβ^{WT}-reconstituted MEFs. In contrast, only IKKα associated with NEMO in IKKβ$^{-/-}$ and IKKβ$^{\Delta NBD}$-reconstituted cells. When immunoprecipitations were performed using anti-IKKα, both NEMO and IKKβ co-precipitated with IKKα from WT, IKKβ^{WT}, and IKKβ$^{\Delta NBD}$ MEFs, whereas only NEMO associated with IKKα in IKKβ$^{-/-}$ cells (Fig. 2*B*). Immunoprecipitation using anti-IKKβ pulled down all three IKK complex sub-

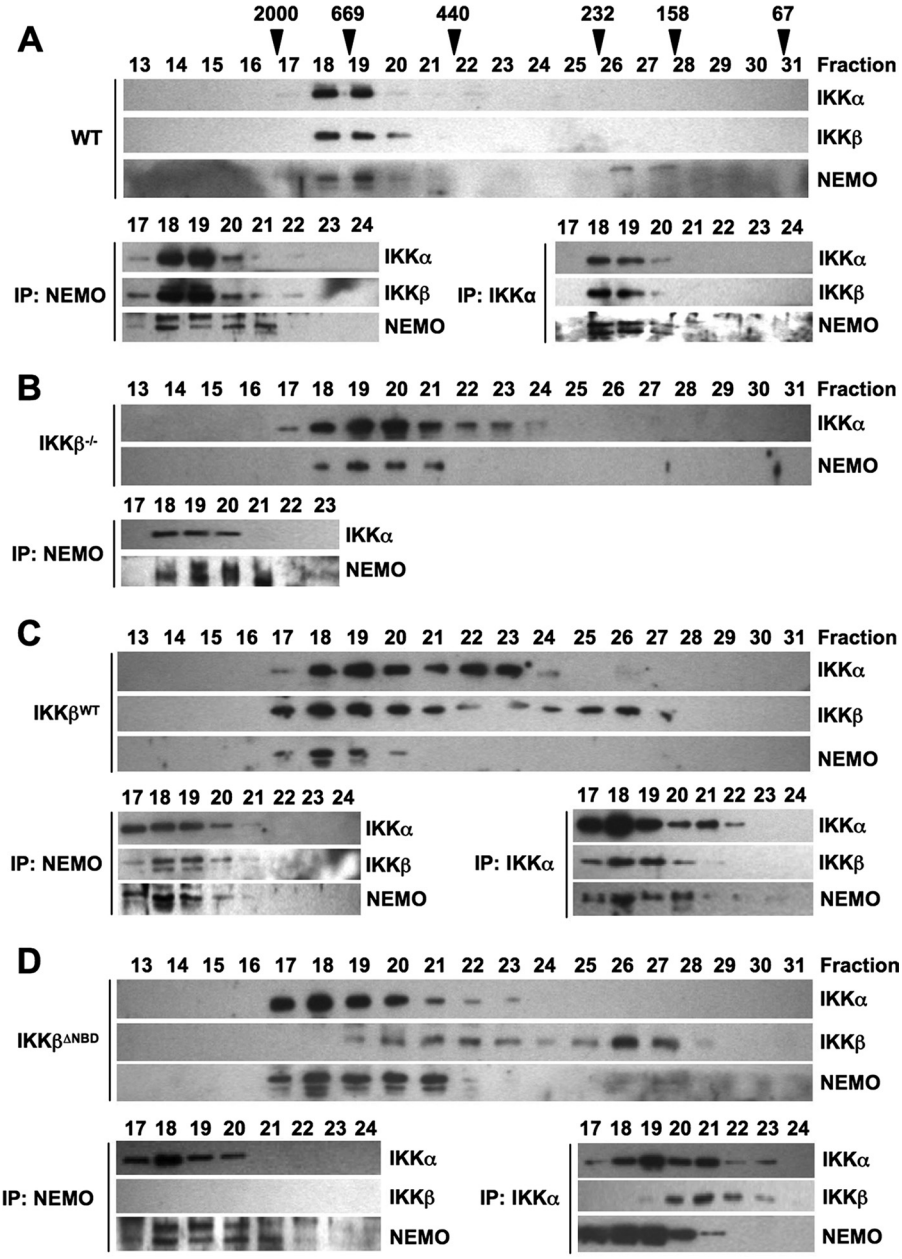

FIGURE 3. **IKKβ$^{\Delta NBD}$ is not incorporated into the tripartite IKK complex.** S100 extracts from WT (*A*), IKKβ$^{-/-}$ (*B*), IKKβ^{WT} (*C*), and IKKβ$^{\Delta NBD}$ MEFs (*D*) were fractionated by size exclusion chromatography. Fractions were immunoblotted using the antibodies indicated (*left*). The column was precalibrated, and the molecular weights of standard proteins are indicated *above* the appropriate fractions in *A*. Fractions containing the high molecular weight IKK complex were immunoprecipitated (*IP*) using either anti-NEMO or anti-IKKα. The resulting immunoblots from these immunoprecipitations are displayed *below* the fractionation profile for each cell type in *A–D*.

units from WT and IKKβ^{WT}-reconstituted MEFs, but as expected, anti-IKKβ did not precipitate any of these proteins from IKKβ$^{-/-}$ cells (Fig. 2*C*, *lane 2*). Intriguingly, anti-IKKβ pulled down complexes consisting of IKKβ$^{\Delta NBD}$ and IKKα but not NEMO from IKKβ$^{\Delta NBD}$-reconstituted MEFs (Fig. 2*C*, *lane 4*). These findings therefore suggest that reconstituted IKKβ^{WT} is incorporated into the heterotrimeric and IKK complex, whereas IKKβ$^{\Delta NBD}$ associates only with endogenous IKKα in a separate complex that does not contain NEMO.

To further explore the nature of the IKK complexes in the reconstituted cell lines, we performed size exclusion chromatography of S100 lysates. As shown in Fig. 3*A* (*top*), and consistent with previous reports (10, 34, 36, 37), IKKα, IKKβ, and NEMO in WT MEFs co-eluted in fractions corresponding to a predicted molecular mass of 600–900 kDa. Immunoprecipitation of complexes from these fractions using anti-NEMO or anti-IKKα confirmed that all three subunits co-precipitated, with the majority of the IKK holocomplex appearing in fractions 18 and 19 (Fig. 3*A*, *bottom*). Fractionation of lysates from IKKβ$^{-/-}$ cells showed that IKKα and NEMO elute together in fractions 18–21, suggesting a complex of ~500–900 kDa (Fig. 3*B*; *top*). In addition, IKKα eluted in fractions 22–24, which did not contain any NEMO. Immunoprecipitation of complexes from fractions 17–23 using anti-NEMO demonstrated association of IKKα with NEMO in fractions 18–21 (Fig. 3*B*, *bottom*). These data therefore demonstrate that in IKKβ$^{-/-}$ MEFs, an IKK complex consisting of only NEMO and IKKα exists that is similar in size to the tripartite complex in WT cells. In addition, a portion of IKKα does not associate with NEMO in the absence of IKKβ but instead elutes in fractions corresponding to a lower molecular weight NEMO-independent complex.

All three IKK complex subunits eluted in high molecular weight fractions (fractions 17–20) in IKKβ^{WT}-reconstituted IKKβ$^{-/-}$ MEFs (Fig. 3*C*, *top*), and immunoprecipitation demonstrated that IKKα, IKKβ, and NEMO associate in these fractions (Fig. 3*C*, *bottom*). Similar to IKKβ$^{-/-}$ cells, IKKα also appeared in fractions 21–24, which did not contain NEMO, and NEMO-IKKα complexes could not be immunoprecipitated in these fractions. Hence, reconstituted IKKβ^{WT} incorporates into the high molecular weight tripartite IKK holocomplex in IKKβ$^{-/-}$ MEFs, and lower molecular weight endogenous IKKα-containing complexes are also detected in these cells. We also consistently observed IKKβ in later eluting fractions up to sample number 27. IKKβ in these fractions was not associated with either IKKα or NEMO (Fig. 3*C*, *bottom*) (data not shown), suggesting that it is an IKKβ homodimeric complex possibly resulting from the high level of overexpression in these cells (Fig. 1*B*).

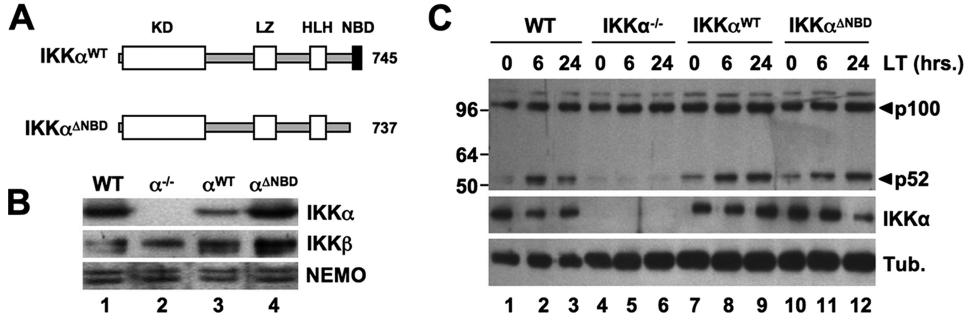

FIGURE 4. **The IKKα NBD is not required for noncanonical NF-κB activation.** *A*, the structural domains of wild-type IKKα (IKKα^{WT}) and IKKα$^{\Delta NBD}$ are shown. *KD*, kinase domain; *LZ*, leucine zipper; *HLH*, helix-loop-helix. IKKα$^{\Delta NBD}$ is a truncation mutant encompassing residues 1–737 that lacks the C-terminal 8 amino acids containing the NBD (13, 14). *B*, lysates from WT, IKKα$^{-/-}$ (α$^{-/-}$), IKKα^{WT} (α^{WT}), and IKKα$^{\Delta NBD}$ (α$^{\Delta NBD}$) MEFs were immunoblotted using the antibodies indicated (*right*). *C*, WT, IKKα$^{-/-}$, IKKα^{WT}, and IKKα$^{\Delta NBD}$ MEFs were either untreated or incubated with LTα1β2 (*LT*) for the times indicated, and then lysates were immunoblotted using either anti-p100/p52 (*top*), anti-IKKα, or anti-tubulin (*Tub.*) as indicated (*right*).

Similar to IKKβ$^{-/-}$ MEFs, IKKα and NEMO eluted together in fractions 17–21 in IKKβ$^{\Delta NBD}$ cell lysates, suggesting that they exist as a complex comparable in size with native IKK in WT MEFs (Fig. 3*D*, *top*). IKKβ$^{\Delta NBD}$ did not co-elute with the majority of IKKα and NEMO but instead eluted in two pools with peaks in fractions 20–22 and 26–27, respectively. The first pool of IKKβ$^{\Delta NBD}$ co-eluted with IKKα in fractions 19–23, whereas the second pool did not co-elute with either IKKα or NEMO. When immunoprecipitations were performed using anti-NEMO (Fig. 3*D*, *bottom*), IKKα but not IKKβ$^{\Delta NBD}$ associated with NEMO in the high molecular weight fractions. Similarly, NEMO co-precipitated with anti-IKKα in fractions 17–21, but IKKβ$^{\Delta NBD}$ only associated with IKKα in fractions 20–23.

Collectively, these data support our findings in Fig. 2 and demonstrate that reconstituted IKKβ$^{\Delta NBD}$ does not incorporate into the tripartite IKK complex in IKKβ$^{-/-}$ MEFs. In these cells, IKKα and NEMO form the high molecular weight IKK complex, whereas IKKβ$^{\Delta NBD}$ associates with IKKα in a separate NEMO-independent complex. In addition, IKKβ$^{\Delta NBD}$ appears in a third, lower molecular weight complex that does not contain either IKKα or NEMO.

IKKα$^{\Delta NBD}$ Restores Noncanonical NF-κB Signaling in IKKα$^{-/-}$ MEFs—To establish the effects of selectively disrupting the IKKα-NEMO interaction on NF-κB signaling and IKK complex formation, we generated retroviral constructs encoding both WT IKKα and a truncation mutant (residues 1–745) lacking the NBD (IKKα$^{\Delta NBD}$) (Fig. 4*A*) and used these to stably transduce IKKα-deficient MEFs. Immunoblotting demonstrated that the cells were reconstituted with IKKα^{WT} and IKKα$^{\Delta NBD}$ (Fig. 4*B*), and FACS analysis confirmed that over 95% of the cells were stably transduced with each construct (not shown). The levels of IKKα^{WT} and IKKα$^{\Delta NBD}$ in multiple stable cells lines generated were consistently similar to those of endogenous IKKα in WT MEFs.

Noncanonical NF-κB signaling requires IKKα but is intact in NEMO-deficient cells (18–20, 22). However, it remains unclear whether disrupting the IKKα NBD in cells containing NEMO affects noncanonical signaling. To address this question, we incubated our panel of MEFs with heterotrimeric lymphotoxin (LTα1β2) and then immunoblotted the resulting lysates using anti-p100/p52. As shown in Fig. 4*C* (*lanes 1–3*), LTα1β2 induced the appearance of p52 in WT MEFs, indicating activation of the noncanonical pathway. As expected, p52 was absent in LTα1β2-stimulated IKKα$^{-/-}$ cells (*lanes 4–6*) but was present in IKKα^{WT}-reconstituted MEFs (*lanes 7–9*). Similarly, IKKα$^{\Delta NBD}$ reconstitution of IKKα$^{-/-}$ MEFs restored LTα1β2-induced p100 processing to p52, demonstrating that the IKKα NBD is not required for noncanonical NF-κB activation.

IKKα$^{\Delta NBD}$ Rescues Classical NF-κB Activity in IKKα$^{-/-}$ MEFs—We next questioned whether loss of the IKKα NBD affects proinflammatory cytokine-induced classical NF-κB activation. Since our earlier study demonstrated that a NEMO-IKKα complex facilitates IL-1-induced classical NF-κB activation (30), we asked whether IKKα$^{\Delta NBD}$ might function as a dominant negative inhibitor of IL-1 signaling. However, consistent with our findings with IKKβ$^{\Delta NBD}$ (Fig. 1*C*), both IL-1 and TNF induced IκBα degradation in IKKα^{WT}- and IKKα$^{\Delta NBD}$-reconstituted MEFs (Fig. 5*A*). Hence, IKKα$^{\Delta NBD}$ does not inhibit the ability of IKKβ to phosphorylate IκBα, leading to its degradation.

Although TNF- and IL-1-induced IκBα degradation is intact in IKKα$^{-/-}$ cells, we found previously that DNA binding of nuclear NF-κB in response to IL-1 is diminished in the absence of IKKα compared with either wild-type or IKKβ$^{-/-}$ MEFs (30). To determine whether IKKα^{WT} or IKKα$^{\Delta NBD}$ could rescue defective NF-κB activation in IKKα-deficient MEFs, we performed EMSAs using our panel of cells. As shown in Fig. 5*B*, IL-1-induced NF-κB activation was maximal in WT MEFs after 15 min and returned to basal levels by 60 min (*lanes 1–4*). Consistent with our previous data (30), DNA binding in IKKα$^{-/-}$ MEFs was less robust than that observed in WT MEFs (compare *lanes 1–4* and *5–8*). However, reintroduction of either IKKα^{WT} or IKKα$^{\Delta NBD}$ into IKKα$^{-/-}$ MEFs restored IL-1-induced NF-κB DNA binding to WT levels (Fig. 5*B*; *lanes 9–16*). Surprisingly, we also found that TNF-induced NF-κB activation was diminished in IKKα$^{-/-}$ MEFs (Fig. 5*C*, *lanes 1–8*), and similar to IL-1 signaling, this defect was rescued by reintroduction of either IKKα^{WT} or IKKα$^{\Delta NBD}$ (*lanes 9–16*).

Previous studies have demonstrated that IKKα enters the nucleus and regulates NF-κB transcriptional activity via mechanisms including phosphorylation of p65 and histone H3 (24–29, 38). We therefore performed NF-κB-dependent luciferase reporter assays to determine the effects of deleting the IKKα NBD on transcriptional activation of NF-κB. Confirming earlier reports (24, 29, 38), we found that neither IL-1 nor TNF could activate NF-κB-dependent transcription in IKKα$^{-/-}$ MEFs (Fig. 5*D*). Stable re-expression of IKKα^{WT} led to an increase in basal transcriptional activity compared with WT MEFs but also rescued the ability of IL-1 and TNF to up-regulate transcription in these cells (Fig. 5*D*). Furthermore, IKKα$^{\Delta NBD}$ also restored basal and cytokine-induced NF-κB

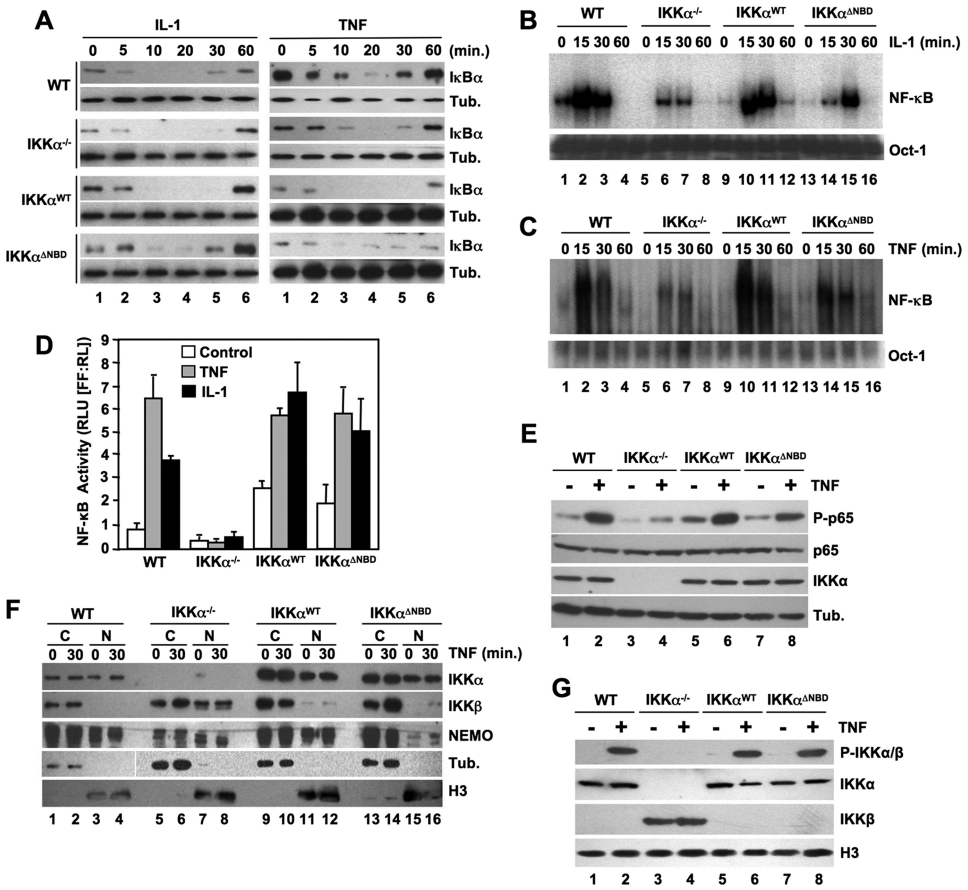

FIGURE 5. **IKKα$^{\Delta NBD}$ restores NF-κB-dependent transcriptional activity.** *A*, WT, IKKα$^{-/-}$, IKKα^{WT}, and IKKα$^{\Delta NBD}$ MEFs were treated with either IL-1α (10 ng/ml) (*left*) or TNF (10 ng/ml) (*right*) for the times indicated, and then lysates were immunoblotted using anti-IκBα or anti-tubulin (*Tub.*) as indicated (*right*). The same panel of MEFs was treated with either IL-1a (*B*) or TNF (*C*) for the times indicated, and then nuclear extracts were prepared for EMSA. Assays were performed using either a consensus NF-κB binding site probe (*top*) or an Oct1 probe as a loading control (*bottom*). *D*, WT, IKKα$^{-/-}$, IKKα^{WT}, and IKKα$^{\Delta NBD}$ MEFs were transiently transfected with the NF-κB-dependent firefly luciferase reporter construct pBIIx-luc together with a control *Renilla* luciferase construct. Twenty-four hours later, cells were either left untreated (*Control*) or treated with IL-1α or TNF for 5 h, and then NF-κB activity was determined by dual luciferase assay. *E*, the MEF panel was either untreated (−) or incubated with TNF for 30 min (+), and then whole cell lysates were immunoblotted using anti-phospho-p65 (*P-p65*), anti-p65, anti-IKKα, and anti-tubulin (*Tub.*), as indicated (*right*). *F*, WT, IKKα$^{-/-}$, IKKα^{WT}, and IKKα$^{\Delta NBD}$ MEFs were either untreated or stimulated for 30 min with TNF, and then nuclear (*N*) and cytoplasmic (*C*) extracts were prepared and immunoblotted using the antibodies indicated (*right*). The integrity of the cytoplasmic and nuclear extracts was confirmed using anti-tubulin and anti-histone H3, respectively. *G*, MEFs were either untreated (−) or stimulated for 30 min with TNF (+), and then nuclear extracts were prepared and immunoblotted using anti-phospho-IKKα/β (P-IKKα/β), anti-IKKα, anti-IKKβ, and anti-histone H3 as indicated (*right*).

transcriptional activity to the same level as that observed in IKKα^{WT}-reconstituted cells (Fig. 5*D*).

Since the ability of IKKα to regulate NF-κB-dependent transcription has been shown to involve phosphorylation of p65 at Ser^{536} (28, 38, 39), we immunoblotted cell lysates using an antibody that recognizes phosphorylated Ser^{536} on p65. As shown in Fig. 5*E*, Ser^{536} phosphorylation in response to TNF was severely diminished in IKKα$^{-/-}$ cells, whereas re-expression of either IKKα^{WT} or IKKα$^{\Delta NBD}$ restored TNF-induced p65 phosphorylation to levels similar to that in WT MEFS (Fig. 5*E*).

In addition to IKKα, NEMO has also been shown to shuttle between the cytoplasm and nucleus (40–43). We therefore questioned whether the ability of IKKα to enter the nucleus, where it regulates NF-κB transcriptional activity, requires its association with NEMO. As shown in Fig. 5*F* (*top*), IKKα was present in the nucleus of untreated WT, IKKα^{WT}, and IKKα$^{\Delta NBD}$ MEFs, and neither TNF nor IL-1 (not shown) stimulation further enhanced its nuclear localization. Furthermore, NEMO was present in the nucleus in WT, IKKα$^{-/-}$, and IKKα^{WT} MEFs but was severely depleted in the nucleus of IKKα$^{\Delta NBD}$ cells. As previously shown (24, 29), IKKβ was absent in the nucleus of WT cells. Surprisingly, however, we detected elevated nuclear IKKβ in IKKα$^{-/-}$ MEFs that was significantly diminished following reconstitution with either IKKα^{WT} or IKKα$^{\Delta NBD}$. Notably, NEMO was also present in the nucleus of IKKα$^{-/-}$ MEFs.

To determine whether nuclear IKKα in the reconstituted cells is activated in response to proinflammatory stimuli, we immunoblotted nuclear lysates using a phospho-specific antibody that recognizes both IKKα and IKKβ only when they are phosphorylated on crucial serines within their catalytic activation loops. As shown in Fig. 5*G*, this antibody detected phosphorylated IKKα in WT, IKKα^{WT}, and IKKα$^{\Delta NBD}$ cells, demonstrating that IKKα in the nuclei of these cells is activated in response to TNF. However, although IKKβ was present in the nucleus of IKKα$^{-/-}$ cells (Fig. 5*G*, *lanes 3* and *4*), we did not detect its phosphorylation, suggesting that nuclear IKKβ is not activated in response to TNF.

Taken together, the findings in Fig. 5 strongly support a model in which the transcriptional regulatory activity of IKKα is independent of its function as a NEMO-associated IκB kinase. Our data also suggest that the ability of IKKα to enter the nucleus and become activated in response to proinflammatory cytokines is NEMO-independent, whereas normal nuclear localization of NEMO requires an intact IKKα NBD. Finally, these results indicate that IKKβ can enter the nucleus but only in the absence of IKKα.

IKKα$^{\Delta NBD}$ Is Not Incorporated into the IKK Holocomplex—To determine whether IKKα$^{\Delta NBD}$ was incorporated into the IKK holocomplex we immunoprecipitated IKK complexes from WT, IKKα$^{-/-}$, IKKα^{WT}, and IKKα$^{\Delta NBD}$ MEFs using anti-NEMO and anti-IKKα. As shown in Fig. 6*A*, IKKα and IKKβ both co-immunoprecipitated with anti-NEMO from WT and IKKα^{WT}-reconstituted MEFs, whereas only IKKβ associated with NEMO in IKKα$^{-/-}$ and IKKα$^{\Delta NBD}$ cells. When anti-IKKα was used for immunoprecipitations, both NEMO and IKKβ co-precipitated with IKKα from WT and IKKα^{WT} MEFs (Fig.

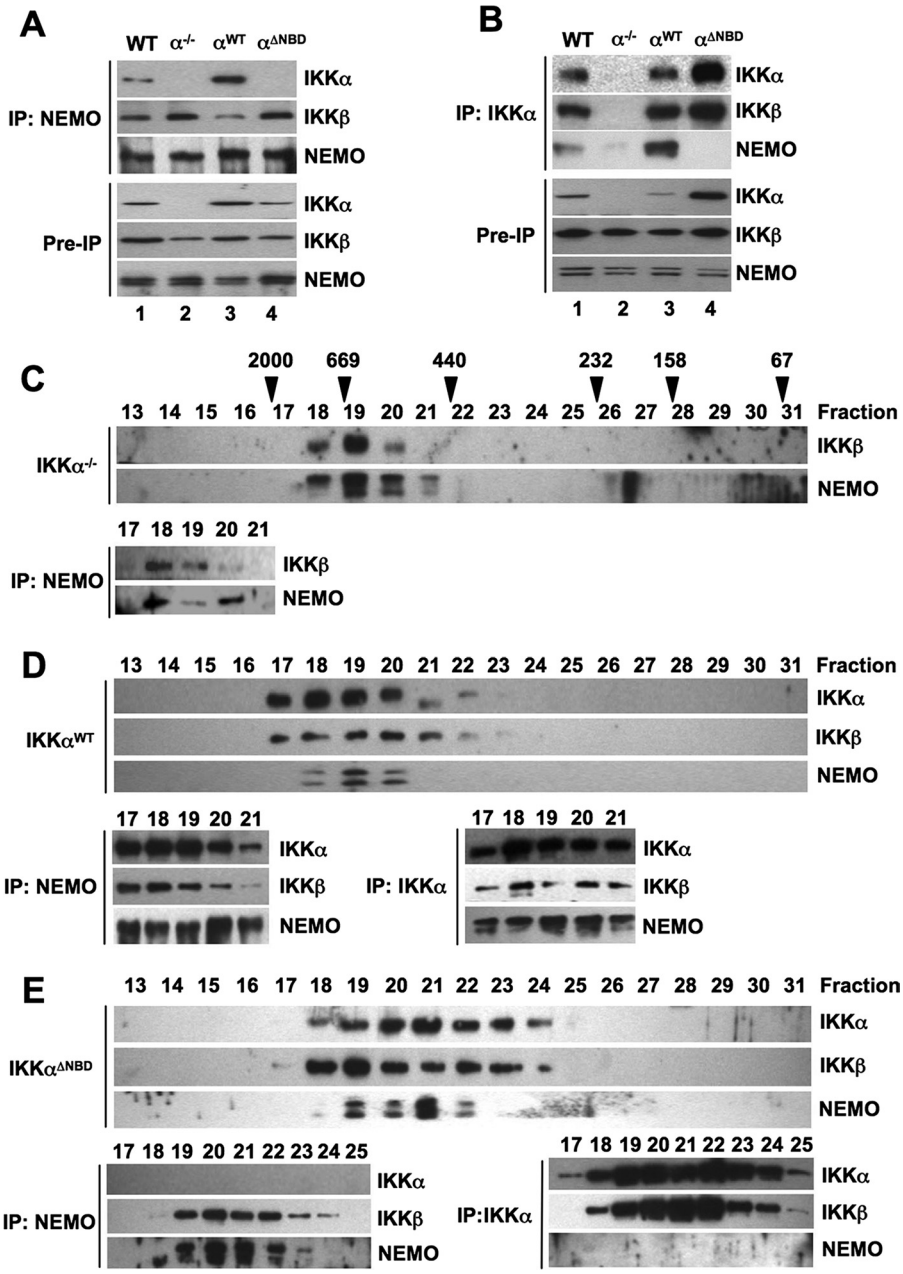

FIGURE 6. **IKKα$^{\Delta NBD}$ is not incorporated into the tripartite IKK complex.** *A* and *B*, IKK complexes in whole cell lysates of wild-type (WT), IKKα$^{-/-}$ (α$^{-/-}$), IKKα^{WT} (α^{WT}), and IKKα$^{\Delta NBD}$ (α$^{\Delta NBD}$) MEFs were immunoprecipitated (*IP*) using anti-NEMO (*A*) or anti-IKKα (*B*). Immunoprecipitated material was immunoblotted using anti-IKKα, anti-IKKβ, and anti-NEMO as indicated (*right*). Samples of lysates saved prior to immunoprecipitation (*Pre-IP*) were immunoblotted using anti-IKKα, anti-IKKβ, and anti-NEMO as shown. *C–E*, S100 extracts from IKKα$^{-/-}$ (*C*), IKKα^{WT} (*D*), and IKKα$^{\Delta NBD}$ (*E*) MEFs were fractionated by size exclusion chromatography. Fractions were immunoblotted using the antibodies indicated (*left*). The column was precalibrated, and the molecular weights of standard proteins are indicated *above* the appropriate fractions in *C*. Fractions containing the high molecular weight IKK complex were immunoprecipitated using either anti-NEMO or anti-IKKα. The resulting immunoblots from these immunoprecipitations are displayed *below* the fractionation profile for each cell type in *C–E*.

6*B*). In contrast, only IKKβ associated with IKKα$^{\Delta NBD}$, suggesting that IKKα$^{\Delta NBD}$ forms a NEMO-independent complex with endogenous IKKβ (Fig. 6*B*).

To further investigate the complexes formed in the reconstituted cell lines, we performed size exclusion chromatography. Following separation of lysates from IKKα$^{-/-}$ cells, IKKβ and NEMO eluted together in fractions 18–21 (Fig. 6*C*, *top*), and immunoprecipitations using anti-NEMO demonstrated that IKKβ associated with NEMO in these fractions (Fig. 6*C*, *bottom*). This profile suggests a NEMO-IKKβ complex of similar size (500–900 kDa) to the tripartite IKK complex in wild-type MEFs that predominantly eluted in fractions 18 and 19 (Fig. 3*A*). When we reconstituted IKKα$^{-/-}$ MEFs with IKKα^{WT}, the bulk of IKK complexes eluted in fractions 17–20 (Fig. 6*D*, *top*), and immunoprecipitation using either anti-NEMO or anti-IKKα confirmed that these complexes contain IKKα, IKKβ, and NEMO (Fig. 6*D*, *bottom*). Thus, IKKα^{WT} is incorporated into the high molecular weight tripartite IKK complex in IKKα$^{-/-}$ cells.

Fractionation of lysates from IKKα$^{\Delta NBD}$-reconstituted MEFs showed that IKKα$^{\Delta NBD}$, IKKβ, and NEMO elute in a broad range of fractions spanning predicted molecular masses from ~250 to 900 kDa (Fig. 6*E*, *top*). When immunoprecipitations were performed using anti-NEMO, IKKβ but not IKKα$^{\Delta NBD}$ associated with NEMO in fractions 19–24 (Fig. 6*E*, *bottom*). In contrast, when anti-IKKα was used to immunoprecipitate complexes, only IKKβ associated with IKKα$^{\Delta NBD}$ in fractions 18–25, and NEMO was not co-precipitated in these samples. Hence, these data support our findings in Fig. 6, *A* and *B*, and demonstrate that reconstituted IKKα$^{\Delta NBD}$ is not incorporated into the tripartite complex. Instead, similar to IKKβ$^{\Delta NBD}$ in IKKβ$^{-/-}$ MEFs (Figs. 2 and 3), endogenous IKKβ and NEMO form a high molecular weight IKK complex, whereas IKKα$^{\Delta NBD}$ associates with IKKβ in a distinct NEMO-independent complex.

In addition to these complexes, our analysis of nuclear extracts demonstrated that IKKα$^{\Delta NBD}$ exists alone in the nucleus separate from either IKKβ or NEMO (Fig. 5*F*). Furthermore, nuclear IKKα$^{\Delta NBD}$ was active as measured using an anti-phospho-IKKα/β antibody (Fig. 5*G*). Since NEMO is absolutely required for activation of the cytoplasmic IKK complex leading to IκBα phosphorylation (8–10, 12), we questioned whether the NEMO-independent IKKβ-IKKα$^{\Delta NBD}$ complex could be activated in response to IL-1α or TNF. To test this, we immunoprecipitated IKK complexes from cytoplasmic extracts of IKKα$^{\Delta NBD}$ and IKKα^{WT} MEFs using either anti-IKKα or anti-

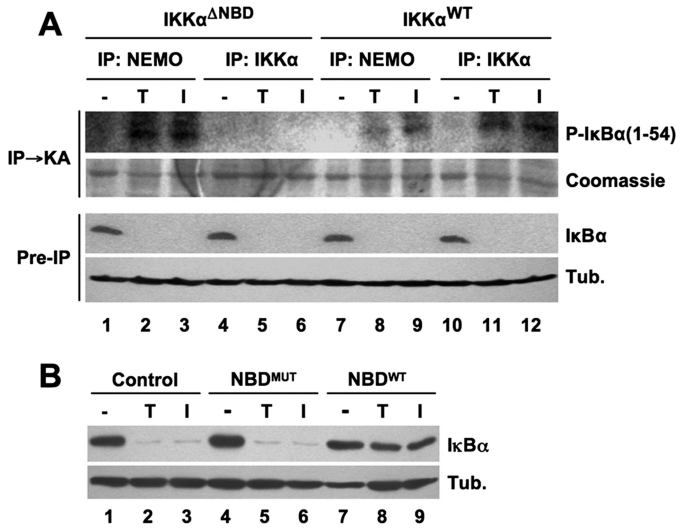

FIGURE 7. **Cytoplasmic IKKα$^{\Delta NBD}$ complexes are not activated by proinflammatory cytokines.** *A*, IKKα$^{\Delta NBD}$ and IKKα^{WT} MEFs were either untreated (−) or incubated for 15 min with either TNF (*T*) or IL-1α (*I*). Cytoplasmic extracts were prepared, and immunoprecipitations (*IP*) were performed using anti-NEMO or anti-IKKα as indicated. The precipitated material was used for an immune complex kinase assay (*IP → KA*) employing glutathione *S*-transferase-fused IκBα 1–54 as a substrate. Phosphorylated IκBα 1–54 (*P-IκBα(1–54)*) was detected by autoradiography, and total substrate was visualized by Coomassie staining. Preimmunoprecipitation (*Pre-IP*) samples from lysates were immunoblotted using anti-IκBα and anti-tubulin (*Tub.*). *B*, IKKα$^{\Delta NBD}$ MEFs were either untreated (*Control*) or incubated for 15 min with either NBD^{MUT} or NBD^{WT} peptide, as indicated. The cells were then incubated a further 15 min in the absence (−) or presence of either TNF (*T*) or IL-1α (*I*). Cytoplasmic lysates were immunoblotted using anti-IκBα and anti-tubulin (*Tub.*) as shown (*right*).

NEMO and then performed immune complex kinase assays using glutathione *S*-transferase-IκBα 1–54 as a substrate. As shown in Fig. 7*A*, immunoprecipitation using anti-NEMO pulled down active IKK complexes from both cell types treated with either TNF or IL-1α (Fig. 7*A*, *lanes 2*, *3*, *8*, and *9*). In contrast, anti-IKKα only precipitated active IKK from IKKα^{WT} MEFs despite the fact that NF-κB signaling was intact in IKKα$^{\Delta NBD}$ cells, as shown by degradation of IκBα (*lanes 4–6*). These findings therefore suggest that the cytoplasmic IKKβ-IKKα$^{\Delta NBD}$ complex in IKKα$^{\Delta NBD}$ cells is not activated in response to cytokines, and it is instead the NEMO-IKKβ alone complex (Fig. 6) that is activated.

To further test this concept, we treated IKKα$^{\Delta NBD}$ cells with the NBD peptide that disrupts the association of NEMO with the IKKs (13, 14). As shown in Fig. 7*B*, the mutant NBD peptide did not affect TNF- or IL-1α-induced IκBα degradation, whereas the wild-type peptide completely blocked IκBα degradation in response to both cytokines. The data in Fig. 7 therefore confirm that NEMO is absolutely required for IκBα degradation in IKKα$^{\Delta NBD}$ cells and demonstrate that the cytoplasmic IKKβ-IKKα$^{\Delta NBD}$ complexes in these cells are not activated by proinflammatory cytokines.

DISCUSSION

The prevailing model of NF-κB signaling suggests that the association of IKKα with NEMO plays no role in classical NF-κB pathway activation (15). However, we demonstrated recently that IKK complexes consisting of only IKKα and NEMO activate classical NF-κB in response to IL-1 (30). In contrast, TNF signaling absolutely requires IKKβ, and the classical NF-κB pathway cannot be activated by TNF in IKKβ-deficient cells (16, 17). Since both IKKα and IKKβ associate with NEMO via their C-terminal NBDs, these findings suggest that the ability of both kinases to bind NEMO regulates their function within the classical signaling pathway. We therefore undertook this study to determine the effects of selectively deleting the NBD in IKKα and IKKβ on TNF- and IL-1-induced NF-κB activation and IKK complex formation. Our findings are summarized in the model depicted in Fig. 8.

Consistent with the stringent requirement for NEMO and IKKβ in TNF signaling (8–12), IKKβ$^{\Delta NBD}$ did not rescue defective TNF-induced IκBα degradation in IKKβ$^{-/-}$ cells. This conclusively demonstrates that direct association of NEMO with IKKβ is absolutely necessary for TNF-induced classical NF-κB activation. Confirming our previous study (30), IL-1-induced IκBα degradation and NF-κB activation was intact in IKKβ$^{-/-}$ MEFs. In light of the failure of IKKβ$^{\Delta NBD}$ to rescue TNF signaling and previous studies demonstrating that IKKβ is a more efficient kinase for IκBα than IKKα (32, 33), we speculated that IKKβ$^{\Delta NBD}$ might function as a dominant negative and block IL-1 signaling. However, reconstitution of IKKβ$^{-/-}$ MEFS with IKKβ$^{\Delta NBD}$ did not affect IL-1-induced IκBα degradation or NF-κB activation. This is in line with our earlier finding that a catalytically inactive IKKβ mutant that blocks TNF signaling did not affect IL-1-induced classical NF-κB activation (30). We therefore conclude that IL-1-induced NEMO-dependent IKKα activation overcomes the potential dominant negative effects of catalytically inactive or NBD-deficient IKKβ. These data underscore the ability of IKKα to either compensate in the absence of IKKβ or function in the presence of defective IKKβ in IL-1- but not TNF-induced classical pathway activation.

Although IKKβ$^{\Delta NBD}$ did not affect IL-1-induced IκBα degradation and NF-κB activation in IKKβ$^{-/-}$ MEFs, NF-κB transcriptional activity was markedly enhanced in IKKβ$^{\Delta NBD}$ cells. IKKβ NEMO binding mutants were shown previously to be constitutively active when overexpressed in HeLa cells (13, 14), and certain deubiquitinases and protein phosphatases that inhibit IKK activity have been reported to associate with NEMO following IKK activation (44–49). Hence, the inability of IKKβ$^{\Delta NBD}$ to recruit these enzymes via NEMO might lead to its increased basal activity. We previously proposed that phosphorylation within the IKKβ NBD is a negative regulatory signal that affects the function of NEMO (13, 14). Several lines of biochemical evidence support this hypothesis (13, 14, 50–53), and Higashimoto *et al.* (51) demonstrated recently that phosphorylation within the NBD by Polo-like kinase down-regulates IKK activity. Notably, however, basal NF-κB activation measured by EMSA was not enhanced in IKKβ$^{\Delta NBD}$ cells, suggesting that additional regulatory signals control IKK and NF-κB transcriptional activity. In this regard, CUEDC2 was shown recently to directly associate with IKKα and IKKβ to inhibit their activity, and this probably occurs in the absence of NEMO (54). Clearly, further work is required to understand fully the mechanisms that deactivate the IKK complex; however, these accumulated findings suggest that both NEMO-dependent and -independent mechanisms exist to accomplish this.

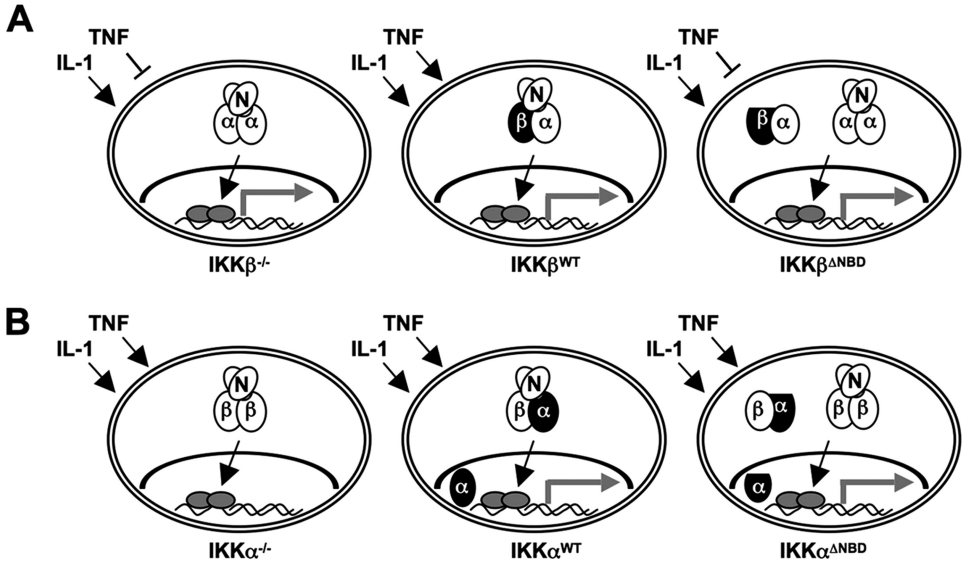

FIGURE 8. **Classical NF-κB signaling and IKK complex formation in IKK-reconstituted cells.** Endogenous proteins are shown as *open ovals* (*N*, NEMO; α, IKKα; β, IKKβ), and reconstituted IKKα and IKKβ are depicted in *black*. IKKα$^{\Delta NBD}$ and IKKβ$^{\Delta NBD}$ are *flattened* to indicate deletion of the NBD. Activated NF-κB is shown as *gray ovals*, and the *gray arrows* indicate transcriptional activity. *A*, IKKβ$^{-/-}$ MEFs (*left*) contain NEMO-IKKα complexes that activate classical NF-κB in response to IL-1 (*arrow*) but not TNF (*blunt-ended line*). Reconstituted IKKβ^{WT} forms a heterotrimeric IKK complex with endogenous NEMO and IKKα and rescues TNF signaling (*middle*). In contrast, IKKβ$^{\Delta NBD}$ neither affects IL-1 signaling nor rescues TNF signaling (*right*). IKKβ$^{\Delta NBD}$ is not incorporated into the heterotrimeric IKK complex but forms complexes with endogenous IKKα that do not contain NEMO. *B*, IKKα$^{-/-}$ MEFs contain NEMO-IKKβ complexes that activate classical signaling (*i.e.* IκBα degradation and NF-κB nuclear localization) in response to TNF and IL-1; however, NF-κB transcriptional activity is defective in these cells (*left*). IKKα^{WT} (*middle*) and IKKα$^{\Delta NBD}$ (*right*) both rescue transcriptional activity, demonstrating that association with NEMO is not required for the ability of IKKα to regulate transcription. IKKα^{WT} forms a heterotrimeric IKK complex with endogenous NEMO and IKKβ, and a portion of IKKα^{WT} enters the nucleus (*middle*). IKKα$^{\Delta NBD}$ is not incorporated into the heterotrimeric IKK complex but instead forms NEMO-independent complexes with endogenous IKKβ (*right*). Nuclear localization of IKKα does not require NEMO association as IKKα$^{\Delta NBD}$ enters the nucleus.

The noncanonical NF-κB pathway requires IKKα and can be activated in the absence of either IKKβ or NEMO (18–20, 22). We confirmed this by rescuing defective lymphotoxin-β receptor-induced p100 processing in IKKα$^{-/-}$ MEFs with IKKα. Moreover, IKKα$^{\Delta NBD}$ also rescued p100 processing, providing further evidence that the association of IKKα with NEMO plays no role in noncanonical pathway activation. We therefore conclude that disrupting the interaction of NEMO with the IKKs selectively blocks the classical pathway and does not affect noncanonical NF-κB signaling. This strongly supports the potential use of the NBD peptide or other pharmacological strategies targeting this interaction as highly specific inhibitors of the classical NF-κB pathway (5, 13, 14, 35).

Consistent with our earlier findings (30) and those of others (17, 55), IL-1 and TNF-induced IκBα degradation was intact in IKKα-deficient cells. Furthermore, IKKα$^{\Delta NBD}$ did not block either TNF- or IL-1-induced IκBα degradation, demonstrating that IKKα$^{\Delta NBD}$ does not function as a dominant negative inhibitor of IKKβ. Together with the effects of re-expressing IKKβ$^{\Delta NBD}$ in IKKβ$^{-/-}$ MEFs described above, this provides further support for our previously proposed model of classical pathway activation (30). In this model, TNF signaling absolutely requires IKKβ associated with NEMO, whereas IL-1 is less stringent and utilizes NEMO with either IKKα or IKKβ to phosphorylate IκBα (30).

Although IL-1 and TNF both induced IκBα degradation in IKKα$^{-/-}$ cells, neither cytokine activated NF-κB transcriptional activity in the absence of IKKα. In addition, DNA binding of nuclear NF-κB was significantly reduced in IKKα-deficient cells. These observations confirm previous reports describing critical roles for IKKα in directly phosphorylating and regulating the transcriptional activity of NF-κB proteins as well as transcriptional co-activators, co-repressors, and histones (24–28, 56). Consistent with these functions, IKKα^{WT} rescued full DNA binding and transcriptional activity in IKKα$^{-/-}$ cells, and intriguingly, activity was also rescued by IKKα$^{\Delta NBD}$. Furthermore, both IKKα^{WT} and IKKα$^{\Delta NBD}$ rescued TNF- and IL-1α-induced phosphorylation of p65, which is severely diminished in IKKα$^{-/-}$ cells. This therefore demonstrates that association with NEMO is not required for IKKα to regulate the transcriptional activity of NF-κB that occurs, at least in part, via phosphorylation of p65.

The ability of IKKα to regulate NF-κB transcriptional activity depends on its capacity to enter the nucleus (24–28, 56). It has also been shown that NEMO shuttles in and out of the nucleus and plays a key role in DNA damage-induced NF-κB activation (40–42, 57). In addition, NEMO regulates transcription by binding to CBP at NF-κB-dependent promoters (43). We therefore questioned whether nuclear translocation of NEMO requires its association with IKKα and whether nuclear IKKα activity requires NEMO. As previously described, IKKα and NEMO, but not IKKβ, were present in the nuclei of WT MEFs (24, 29); however, cytokine-stimulation did not affect the nuclear levels of either of these proteins. TNF stimulation activated nuclear IKKα in WT MEFs and also activated IKKα that was present in the nuclei of both IKKα^{WT} and IKKα$^{\Delta NBD}$ cells. Since our immune complex kinase analysis demonstrated that cytoplasmic IKKα$^{\Delta NBD}$ complexes cannot be activated, these findings strongly suggest that IKKα activation occurs in the nucleus. Further work is clearly required to determine the precise mechanisms of activation of nuclear IKKα; however, our data demonstrate that this occurs independently of its association with NEMO.

Surprisingly, we found IKKβ and NEMO in the nucleus of IKKα$^{-/-}$ cells. Unlike IKKα, IKKβ does not contain a nuclear localization sequence, suggesting that in the absence of IKKα, NEMO chaperones IKKβ into the nucleus (28). Notably, and in contrast to nuclear IKKα, we did not detect any TNF-induced activation of nuclear IKKβ in IKKα$^{-/-}$ cells. When we re-expressed IKKα^{WT} in IKKα$^{-/-}$ cells, the cytoplasmic and nuclear distribution of IKKα, IKKβ, and NEMO was identical to that in

WT MEFs, demonstrating that IKKα maintains these homeostatic levels. Furthermore, in IKKα$^{\Delta NBD}$-reconstituted MEFs we found IKKα in the nucleus in the absence of significant levels of NEMO. Taken together, these findings demonstrate that although NEMO binding is not required for IKKα to enter the nucleus and regulate NF-κB transcription, the IKKα NBD is critical for NEMO nuclear localization in cells containing IKKα. Future efforts to fully dissect the mechanisms regulating nuclear localization of the separate IKK complex subunits are necessary, but our findings suggest that these mechanisms are not mutually exclusive.

IKKα and IKKβ associate via interactions between their respective leucine zipper domains (34), and the most abundant form of the IKK complex is a heterodimer of IKKα and IKKβ associated with NEMO (1, 6, 7). This suggests that IKK heterodimerization is the preferential conformation for the IKKs, although IKK homodimeric complexes have been reported (9, 58, 59). We predicted that ΔNBD versions of IKKα and IKKβ re-expressed in knock-out MEFs would heterodimerize with the endogenous partner kinase containing an intact NBD. We further reasoned that NEMO would associate via this endogenous NBD and that the resulting complex would consist of the re-expressed IKK$^{\Delta NBD}$, the endogenous IKK, and endogenous NEMO. Consistent with this notion, immunoprecipitation and gel filtration analysis confirmed that IKKα^{WT} and IKKβ^{WT} re-expressed in IKKα$^{-/-}$ and IKKβ$^{-/-}$ MEFs, respectively, formed heterotrimeric complexes with endogenous IKKs and NEMO (see model in Fig. 8). In contrast, although IKKα$^{\Delta NBD}$ and IKKβ$^{\Delta NBD}$ associated with endogenous IKKβ and IKKα, respectively, these heterodimers did not bind to NEMO despite the presence of an intact NBD on the endogenous kinase. Furthermore, our immune complex kinase assay and NBD peptide experiments clearly demonstrate that in IKKα$^{\Delta NBD}$ cells, the IKKβ-IKKα$^{\Delta NBD}$ complex is not activated by IL-1α or TNF, and it is the NEMO-IKKβ complex that responds to stimulation. Consequently, these findings demonstrate that in the absence of one NBD, the heterotrimeric IKK holocomplex cannot assemble, and the resulting NEMO-independent complexes do not respond to proinflammatory cytokine signaling.

Recent reports have revealed that NEMO forms dimers through interactions between specific domains within the N-terminal region of the protein (35, 60). Furthermore, this portion of NEMO is necessary and sufficient for association with the NBDs of IKKα and IKKβ (13, 35, 52, 60). Recent elegant crystallographic studies revealed that this dimeric conformation of the NEMO N terminus forms two parallel 800-Å α-helical IKK-binding pockets into which the NBDs insert (35). Since the heterodimeric complexes formed between endogenous IKK and re-expressed IKK$^{\Delta NBD}$ did not associate with NEMO, we conclude that the presence of two NBDs is essential for stable formation of this interaction with NEMO. It is intriguing to speculate that the single NBD IKK heterodimer cannot "clamp" into the IKK binding pocket formed by the NEMO dimers; however, extensive structural analysis of these ΔNBD complexes is required to draw any definitive conclusions. Nevertheless, our data suggest that separately targeting the interaction of NEMO with either IKK will disrupt the entire IKK complex.

In conclusion, we have demonstrated that the interaction of NEMO with both IKKs is necessary for classical NF-κB pathway activation and IKK complex assembly. We have further established that IL-1-induced classical NF-κB activation remains intact in cells lacking functional IKKβ. Tremendous effort has been directed toward developing specific inhibitors of IKKβ (3, 4); however, our findings suggest that this strategy may not effectively block all classical NF-κB activation. Importantly, Lam *et al.* (31) demonstrated recently that selective inhibition of IKKβ blocks classical pathway-dependent cell survival in a subtype of diffuse large B-cell lymphoma cells only when IKKα is concomitantly ablated. These accumulated findings therefore support efforts to develop NBD-targeting small molecule inhibitors. Such drugs are predicted to inhibit all classical NF-κB activation while retaining both the noncanonical pathway and the NEMO-independent transcriptional regulatory roles of IKKα intact.

REFERENCES

1. Hayden, M. S., and Ghosh, S. (2008) *Cell* **132,** 344–362
2. Karin, M. (2006) *Nature* **441,** 431–436
3. Gilmore, T. D., and Herscovitch, M. (2006) *Oncogene* **25,** 6887–6899
4. Karin, M., Yamamoto, Y., and Wang, Q. M. (2004) *Nat. Rev. Drug Discov.* **3,** 17–26
5. Orange, J. S., and May, M. J. (2008) *Cell Mol. Life Sci.* **65,** 3564–3591
6. Häcker, H., and Karin, M. (2006) *Sci. STKE 2006*, re13
7. Scheidereit, C. (2006) *Oncogene* **25,** 6685–6705
8. Makris, C., Godfrey, V. L., Krähn-Senftleben, G., Takahashi, T., Roberts, J. L., Schwarz, T., Feng, L., Johnson, R. S., and Karin, M. (2000) *Mol. Cell* **5,** 969–979
9. Mercurio, F., Murray, B. W., Shevchenko, A., Bennett, B. L., Young, D. B., Li, J. W., Pascual, G., Motiwala, A., Zhu, H., Mann, M., and Manning, A. M. (1999) *Mol. Cell Biol.* **19,** 1526–1538
10. Rothwarf, D. M., Zandi, E., Natoli, G., and Karin, M. (1998) *Nature* **395,** 297–300
11. Rudolph, D., Yeh, W. C., Wakeham, A., Rudolph, B., Nallainathan, D., Potter, J., Elia, A. J., and Mak, T. W. (2000) *Genes Dev.* **14,** 854–862
12. Yamaoka, S., Courtois, G., Bessia, C., Whiteside, S. T., Weil, R., Agou, F., Kirk, H. E., Kay, R. J., and Israël, A. (1998) *Cell* **93,** 1231–1240
13. May, M. J., D'Acquisto, F., Madge, L. A., Glöckner, J., Pober, J. S., and Ghosh, S. (2000) *Science* **289,** 1550–1554
14. May, M. J., Marienfeld, R. B., and Ghosh, S. (2002) *J. Biol. Chem.* **277,** 45992–46000
15. Bonizzi, G., and Karin, M. (2004) *Trends Immunol.* **25,** 280–288
16. Li, Q., Van Antwerp, D., Mercurio, F., Lee, K. F., and Verma, I. M. (1999) *Science* **284,** 321–325
17. Li, Z. W., Chu, W., Hu, Y., Delhase, M., Deerinck, T., Ellisman, M., Johnson, R., and Karin, M. (1999) *J. Exp. Med.* **189,** 1839–1845
18. Claudio, E., Brown, K., Park, S., Wang, H., and Siebenlist, U. (2002) *Nat. Immunol.* **3,** 958–965
19. Coope, H. J., Atkinson, P. G., Huhse, B., Belich, M., Janzen, J., Holman, M. J., Klaus, G. G., Johnston, L. H., and Ley, S. C. (2002) *EMBO J.* **21,** 5375–5385
20. Dejardin, E., Droin, N. M., Delhase, M., Haas, E., Cao, Y., Makris, C., Li, Z. W., Karin, M., Ware, C. F., and Green, D. R. (2002) *Immunity* **17,** 525–535
21. Derudder, E., Dejardin, E., Pritchard, L. L., Green, D. R., Korner, M., and Baud, V. (2003) *J. Biol. Chem.* **278,** 23278–23284
22. Senftleben, U., Cao, Y., Xiao, G., Greten, F. R., Krähn, G., Bonizzi, G., Chen, Y., Hu, Y., Fong, A., Sun, S. C., and Karin, M. (2001) *Science* **293,** 1495–1499
23. Madge, L. A., Kluger, M. S., Orange, J. S., and May, M. J. (2008) *J. Immunol.* **180,** 3467–3477
24. Anest, V., Hanson, J. L., Cogswell, P. C., Steinbrecher, K. A., Strahl, B. D., and Baldwin, A. S. (2003) *Nature* **423,** 659–663

25. Hoberg, J. E., Popko, A. E., Ramsey, C. S., and Mayo, M. W. (2006) *Mol. Cell Biol.* **26,** 457–471
26. Hoberg, J. E., Yeung, F., and Mayo, M. W. (2004) *Mol. Cell* **16,** 245–255
27. Huang, W. C., Ju, T. K., Hung, M. C., and Chen, C. C. (2007) *Mol. Cell* **26,** 75–87
28. Lawrence, T., Bebien, M., Liu, G. Y., Nizet, V., and Karin, M. (2005) *Nature* **434,** 1138–1143
29. Yamamoto, Y., Verma, U. N., Prajapati, S., Kwak, Y. T., and Gaynor, R. B. (2003) *Nature* **423,** 655–659
30. Solt, L. A., Madge, L. A., Orange, J. S., and May, M. J. (2007) *J. Biol. Chem.* **282,** 8724–8733
31. Lam, L. T., Davis, R. E., Ngo, V. N., Lenz, G., Wright, G., Xu, W., Zhao, H., Yu, X., Dang, L., and Staudt, L. M. (2008) *Proc. Natl. Acad. Sci. U.S.A.* **105,** 20798–20803
32. Wu, C., and Ghosh, S. (2003) *J. Biol. Chem.* **278,** 31980–31987
33. Zandi, E., Chen, Y., and Karin, M. (1998) *Science* **281,** 1360–1363
34. Zandi, E., Rothwarf, D. M., Delhase, M., Hayakawa, M., and Karin, M. (1997) *Cell* **91,** 243–252
35. Rushe, M., Silvian, L., Bixler, S., Chen, L. L., Cheung, A., Bowes, S., Cuervo, H., Berkowitz, S., Zheng, T., Guckian, K., Pellegrini, M., and Lugovskoy, A. (2008) *Structure* **16,** 798–808
36. DiDonato, J. A., Hayakawa, M., Rothwarf, D. M., Zandi, E., and Karin, M. (1997) *Nature* **388,** 548–554
37. Mercurio, F., Zhu, H., Murray, B. W., Shevchenko, A., Bennett, B. L., Li, J., Young, D. B., Barbosa, M., Mann, M., Manning, A., and Rao, A. (1997) *Science* **278,** 860–866
38. Sizemore, N., Lerner, N., Dombrowski, N., Sakurai, H., and Stark, G. R. (2002) *J. Biol. Chem.* **277,** 3863–3869
39. Sakurai, H., Chiba, H., Miyoshi, H., Sugita, T., and Toriumi, W. (1999) *J. Biol. Chem.* **274,** 30353–30356
40. Berchtold, C. M., Wu, Z. H., Huang, T. T., and Miyamoto, S. (2007) *Mol. Cell Biol.* **27,** 497–509
41. Bredemeyer, A. L., Helmink, B. A., Innes, C. L., Calderon, B., McGinnis, L. M., Mahowald, G. K., Gapud, E. J., Walker, L. M., Collins, J. B., Weaver, B. K., Mandik-Nayak, L., Schreiber, R. D., Allen, P. M., May, M. J., Paules, R. S., Bassing, C. H., and Sleckman, B. P. (2008) *Nature* **456,** 819–823
42. Huang, T. T., Wuerzberger-Davis, S. M., Wu, Z. H., and Miyamoto, S. (2003) *Cell* **115,** 565–576
43. Verma, U. N., Yamamoto, Y., Prajapati, S., and Gaynor, R. B. (2004) *J. Biol. Chem.* **279,** 3509–3515
44. Brummelkamp, T. R., Nijman, S. M., Dirac, A. M., and Bernards, R. (2003) *Nature* **424,** 797–801
45. Fu, D. X., Kuo, Y. L., Liu, B. Y., Jeang, K. T., and Giam, C. Z. (2003) *J. Biol. Chem.* **278,** 1487–1493
46. Hong, S., Wang, L. C., Gao, X., Kuo, Y. L., Liu, B., Merling, R., Kung, H. J., Shih, H. M., and Giam, C. Z. (2007) *J. Biol. Chem.* **282,** 12119–12126
47. Kovalenko, A., Chable-Bessia, C., Cantarella, G., Israël, A., Wallach, D., and Courtois, G. (2003) *Nature* **424,** 801–805
48. Prajapati, S., Verma, U., Yamamoto, Y., Kwak, Y. T., and Gaynor, R. B. (2004) *J. Biol. Chem.* **279,** 1739–1746
49. Zhang, S. Q., Kovalenko, A., Cantarella, G., and Wallach, D. (2000) *Immunity* **12,** 301–311
50. Delhase, M., Hayakawa, M., Chen, Y., and Karin, M. (1999) *Science* **284,** 309–313
51. Higashimoto, T., Chan, N., Lee, Y. K., and Zandi, E. (2008) *J. Biol. Chem.* **283,** 35354–35367
52. Palkowitsch, L., Leidner, J., Ghosh, S., and Marienfeld, R. B. (2008) *J. Biol. Chem.* **283,** 76–86
53. Schomer-Miller, B., Higashimoto, T., Lee, Y. K., and Zandi, E. (2006) *J. Biol. Chem.* **281,** 15268–15276
54. Li, H. Y., Liu, H., Wang, C. H., Zhang, J. Y., Man, J. H., Gao, Y. F., Zhang, P. J., Li, W. H., Zhao, J., Pan, X., Zhou, T., Gong, W. L., Li, A. L., and Zhang, X. M. (2008) *Nat. Immunol.* **9,** 533–541
55. Hu, Y., Baud, V., Oga, T., Kim, K. I., Yoshida, K., and Karin, M. (2001) *Nature* **410,** 710–714
56. Luo, J. L., Tan, W., Ricono, J. M., Korchynskyi, O., Zhang, M., Gonias, S. L., Cheresh, D. A., and Karin, M. (2007) *Nature* **446,** 690–694
57. Wu, Z. H., Shi, Y., Tibbetts, R. S., and Miyamoto, S. (2006) *Science* **311,** 1141–1146
58. Fontan, E., Traincard, F., Levy, S. G., Yamaoka, S., Véron, M., and Agou, F. (2007) *FEBS J.* **274,** 2540–2551
59. Khoshnan, A., Kempiak, S. J., Bennett, B. L., Bae, D., Xu, W., Manning, A. M., June, C. H., and Nel, A. E. (1999) *J. Immunol.* **163,** 5444–5452
60. Marienfeld, R. B., Palkowitsch, L., and Ghosh, S. (2006) *Mol. Cell Biol.* **26,** 9209–9219